Astron. Astrophys. 349, 253–258 (1999)

ASTRONOMY AND ASTROPHYSICS

High resolution Fourier transform spectroscopy of H_2 IR emission in NGC 7023⋆

J.L. Lemaire[1,2], D. Field[3], J.P. Maillard[4], G. Pineau des Forêts[5], E. Falgarone[6], F.P. Pijpers[7], M. Gerin[6], and F. Rostas[5]

[1] Observatoire de Paris-Meudon, F-92195 Meudon Principal Cedex, France
[2] UMR8588 du CNRS, Université de Cergy-Pontoise, F-95806 Cergy Cedex, France
[3] Institute for Storage Ring Facilities, University of Aarhus, DK-8000 Aarhus C, Denmark and UMR8588 du CNRS, Observatoire de Paris-Meudon
[4] UPR341 du CNRS, Institut d'Astrophysique, 98bis, Boulevard Arago, F-75014 Paris, France
[5] UMR8631 du CNRS, Observatoire de Paris-Meudon, F-92195 Meudon Principal Cedex, France
[6] UMR8540 du CNRS, Ecole Normale Supérieure, 24 Rue Lhomond, F-75231 Paris Cedex 05, France
[7] Theoretical Astrophysics Centre, University of Aarhus, DK-8000 Aarhus C, Denmark

Received 22 February 1999 / Accepted 22 June 1999

Abstract. A Fourier transform spectrum at a resolution of $\sim$ 125,000 has been recorded of molecular hydrogen emission in the reflection nebula NGC 7023, in the S(1) v=1-0 line at 2.121 μm for a region 5 arcsec in diameter. The line is resolved and the derived linewidth corresponds to a kinetic temperature of 500$\pm$ 70 K, if all motions are thermal. Comparison with data for HI, CI, CII and CO shows that there is a velocity gradient in the molecular material in the photodissociation region, demonstrating the motion of the photodissociation front relative to the molecular cloud. Models of the photodissociation region experience only limited success in reproducing the known brightness of the H_2 emission in conjunction with the kinetic temperature determined here.

Key words: ISM: clouds – ISM: individual objects: – ISM: kinematics and dynamics – ISM: lines and bands – ISM: molecules – ISM: reflection nebulae

1. Introduction

The reflection nebula NGC 7023 represents an early phase of stellar evolution in which a young star HD 200775, of spectral class B2.5Ve, illuminates and interacts strongly with the remnant of its parent molecular cloud. This photodissociation or "photon-dominated" region (PDR) has been extensively studied, for example in radio (Fuente et al. 1992, 1993, 1996, 1998a; Fuente & Martin-Pintado 1997; Rogers et al. 1995; Gerin et al. 1998), infrared (Sellgren et al. 1992; Lemaire et al. 1996; Martini et al. 1997; Laureijs et al. 1996; Césarsky et al. 1996, Moutou et al. 1998), and visible and UV wavelengths (e.g. Witt et al. 1992, 1993; Murphy et al. 1993; Federman et al. 1997). Reference to work before 1992 may be found in Lemaire et al. 1996.

Photodissociation regions cover a very wide range of conditions, spanning zones of low density of only 100 particles cm^{-3} and low irradiation, to regions of very high density, in excess of 10^6 particles cm^{-3}, with ambient radiation fields many thousands of times that of the average interstellar radiation field. NGC 7023 lies among the high density, high irradiation class of objects, with number densities in the range 10^5 to 10^6 cm^{-3} at the inner border of the irradiated cloud, with a UV radiation field 10^4 times the ambient UV interstellar field (Gerin et al. 1998). Studies to date shed considerable light on the photochemistry, temperature, number density and the dynamics and morphology of NGC 7023 both at the inner illuminated surface of the cloud of gas around HD 200775, and as a function of depth into the cloud, penetrating into the zone in which the direct influence of high energy photons becomes small or negligible.

In the present work we continue our study of H_2 rovibrational emission around 2 μm in NGC 7023, initiated in Lemaire et al. 1996. H_2 emission probes the interface between the ionization zone, the atomic zone and the threshold of the molecular zone (Rogers et al. 1995; Fuente et al. 1996; Gerin et al. 1998). In dense PDRs, the H_2 emitting zone is very thin. For example, PDR models show that gas of density $n_H + 2n_{H_2}$=10^5 cm^{-3} to 10^6 cm^{-3} yields H_2 emission from a zone of thickness of 10^{-3} pc or less. In earlier work we have established something of the morphology of the emitting gas. This shows overall narrow filamentary structure, with small scale structure, that is, clumping, on a scale of 0.004 pc or less. Here we report a high resolution Fourier transform spectrum of a small portion of this emission, without imaging. The object of this work is to investigate the dynamics and temperature of the H_2 emitting zone, through determination for the first time of the H_2 emission linewidth and velocity. Information on the extent of turbulence may be gained from the observed H_2 linewidth and

Send offprint requests to: D. Field

⋆ Visiting astronomers (JPM, JLL, DF, EF) at the Canada-France-Hawaii Telescope, operated by the National Research Council of Canada, the Centre National de la Recherche Scientifique de France and the University of Hawaii

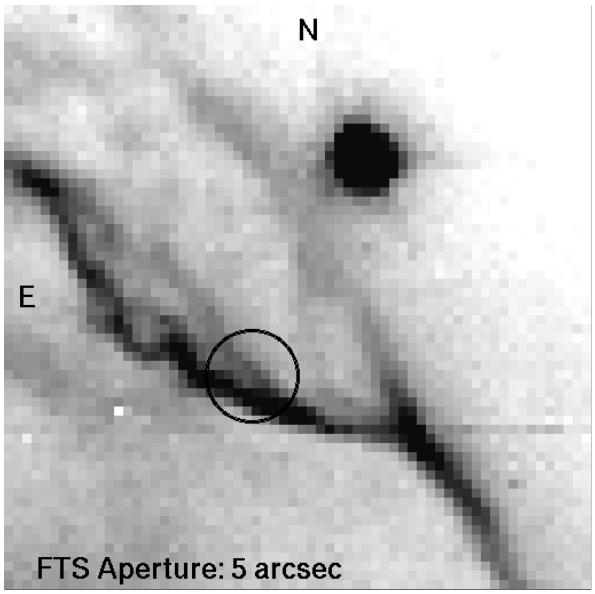

Fig. 1. A grey-scale image of part of the H_2 S(1) v=1-0 IR emission at 2.121 μm recorded in Lemaire et al. 1996. The circle of diameter 5 arcsec shows the position and extent of the region observed in the current work. The illuminating star, HD 200775, lies 48 arcsec to the SE of the centre of the circle marked on the image. HD 200775 itself lies at $\alpha(1950) = 21^h00^m59^s.7$, $\delta(1950) = 67^0 57' 55".5$.

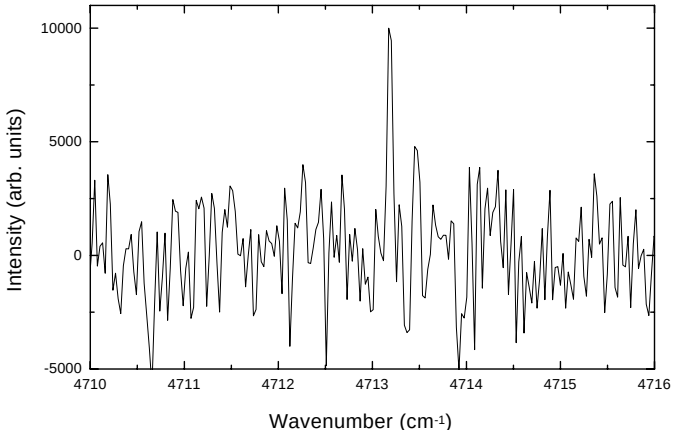

Fig. 2. A 6 cm^{-1} region of the observed spectrum in the vicinity of the H_2 v=1-0 S(1) line

those of other species. A determination of linewidth, translated into temperature, places useful constraints on PDR models, as outlined in Sect. 3.

2. Observations and data reduction

The strongest isolated line in the H_2 IR emission spectrum, by a considerable margin, is the H_2 S(1) v=1-0 IR emission line at 2.121 μm. Images of NGC 7023 (Lemaire et al. 1996) in this line obtained with the Canada-France-Hawaii Telescope (CFHT) showed that the most intense emission lay at a position 32″W and 35.5″N of the exciting star. This is the position to which we point in the present work. To obtain the highest precision in pointing, we have made use of the closer star (the K-star – Sellgren 1983) taking an offset of 12 arcsec S and 6 arcsec E from that position. We set out to obtain as high a resolution spectrum as possible in the wavelength region of the S(1) line at this position. For ease of identification, a grey-scale plot of the H_2 emission reported in Lemaire et al. 1996 is shown in Fig. 1 with a circle to mark the position and extent of the region observed in the current work.

Our observations were performed using the CFHT equipped with the Fourier Transform Spectrometer (FTS). Details of the working of the CFHT FTS may be found in Maillard & Michel 1982. Very briefly, this instrument uses the f/35 infrared focus of the CFHT, with circular apertures whose diameters have been chosen to be 5 arcseconds in this experiment. The FTS is equipped with two such entrance apertures separated by 52 arcseconds, oriented along the EW axis with the Cassegrain bonnette at zero angle. One aperture sampled the H_2 emission region, and the other sampled the sky to the east in a region free of H_2 emission. The sky was therefore automatically subtracted, making use of the fact that the radiation entering the two apertures arrives in antiphase at the detector. Background subtraction is important principally to remove atmospheric contamination, especially from the OH Meinel bands. These bands are both strong and potentially variable through the period of observation (Oliva & Origlia 1992; Abrams et al. 1994). There is otherwise relatively little non-terrestrial sky background in the wavelength range of interest. A filter extending from $\sim$ 4550 cm^{-1} to $\sim$ 4900 cm^{-1} (2.0 μm to 2.2 μm) was used in these observations. A stabilised He-Ne laser controls the path difference in the FTS. The determination of precise wavelengths and the associated accuracy are discussed below.

Observations were carried out on the night of July 27th-28th 1996. For reliable data we required both a good sky for the 4 hours duration of the experiment and a low air-mass, that is, good sky at the correct time of the night. Observations took place between $\sim$ 11:00 pm and $\sim$ 3:00 am local time during which period NGC 7023 was between 58 and 45 degrees above the horizon. A resolution of $\sim$ 125,000 was achieved, that is $\sim$ 2.4 km s^{-1}. This is more than a factor of 5 better than the highest resolution ever achieved before for IR H_2 emission (Burton et al. 1990). The observed spectrum, over a 6 cm^{-1} region in the vicinity of the S(1) line, is shown in Fig. 2. No other lines could confidently be identified as lying outside of the noise within the entire spectral range observed.

Fig. 3 shows experimental points, from Fig. 2, of the S(1) line over a range of 0.27 cm^{-1}. The sampling frequency, set by the FTS step-size, satisfies the Nyquist criterion and the lineshape is therefore well-defined in this spectrum. The lineshape function associated with the interferometer, shown as a dotted line, is a sinc function due to the finite path difference, δ, used in the observations. The sinc function takes the form $\sin(2\pi k.\delta)/(\pi k)$ where k is the wavevector (=$1/\lambda$). Assuming the line profile to be a gaussian, the true lineshape may be determined by convolving a gaussian with the instrumental sinc function in Fig. 3, to obtain the fit shown as a solid line. The

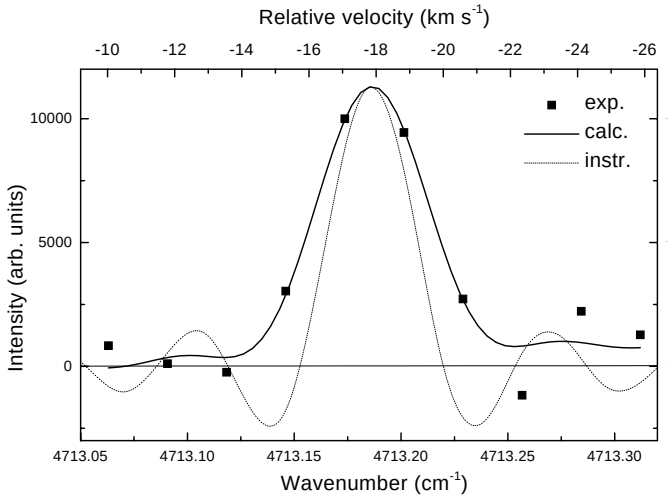

Fig. 3. Experimental data (black squares) showing the H_2 v=1-0 S(1) line over a range of 0.27 cm^{-1}. The dotted line is the lineshape function associated with the interferometer. The solid line is a fit to the observations obtained by convoluting the instrumental lineshape function with a gaussian.

line centre is found to be at 4713.1863± 0.003 cm^{-1} and the full width at half maximum (FWHM) of the line is 53±13 x 10^{-3} cm^{-1}. This linewidth corresponds to 3.4±0.8 km s^{-1} equivalent to a kinetic temperature of 500±70 K, if the width is due to thermal motions only.

Turning to the line centre value, this is blue-shifted by 0.2809 cm^{-1} from the rest frequency, where we have used the value of 4712.9054 cm^{-1} *in vacuo* corresponding to a wavelength of 2.1212544 μm in standard air (Bragg et al. 1982). This blue-shift corresponds to a velocity of -17.88 km s^{-1}, where the standard convention is used that the more negative (or less positive) a velocity, the more relatively blue-shifted is the object. Several corrections must be applied to this raw value. Differential refraction, between the S(1) H_2 and He-Ne line frequencies, for mean conditions on Mauna Kea of 615 mbar, 2^{o}C and 20% relative humidity, leads to a blue-shift of the line by 0.68 km s^{-1}. An aperture correction, arising because the isophase surface is not flat across the 5 arcsec aperture of the FTS, adds a further blue-shift of 0.28 km s^{-1}. In addition, calibration performed during the same observing run was made using CO lines and leads to a red-shift of 0.25 km s^{-1}. This shift, corresponding to 0.0039 cm^{-1}, arises through geometrical effects due to the He-Ne laser alignment. The true velocity shift of the line then becomes -18.59 km s^{-1}. The overall accuracy of this figure is ±0.25 km s^{-1} taking into account both the accuracy of determination of the line position and the accuracy of the calibration corrections.

3. Discussion of results

We seek first to compare the velocity and linewidth of H_2 emission with that of other species, specifically data for CII, CI and CO, reported in Gerin et al. 1998 and Fuente et al. 1998a and HI data reported in Fuente et al. 1996. The velocity shift of the H_2 line is converted into v_{lsr}, the reference frame for radio-data. The earth and heliocentric velocities differ by 8.45 km s^{-1} taking into account the position of the star and the date of observations. Thus v_{helio} of the H_2 emission = -18.59 +8.45 = -10.14 km s^{-1}. The corresponding v_{lsr} for our observed H_2 line is v_{helio} + 13.88 km s^{-1}, that is, +3.75±0.25 km s^{-1}.

A comparison with radio- data is given in Table 1, showing the linewidths and velocities of HI observed with a 14″ beam, CII observed with a 45″ beam, neutral C observed with a 15″ beam, ^{12}CO(6-5) observed with a 10″ beam, ^{13}CO(3-2) observed with a 20″ beam and ^{13}CO(1-0) observed with a 24″ beam. Data in Table 1 have been derived from spectra taken at the same location within the plane of the sky as the data for H_2, so far as possible. Our present H_2 data are included for ease of reference. All velocities shown are v_{lsr}. The velocity of the ^{13}CO J=1-0 emission has been estimated from a velocity-position diagram given in Fuente et al. 1998a.

Turning first to the velocity data shown in Table 1, there is good correspondence between the velocity of HI and of H_2. However other species appear at a different set of velocities and the results in Table 1 show that there is a gradient of velocity from the atomic gas into the molecular gas. Material becomes progressively less red-shifted as we penetrate further into the molecular cloud. The velocity data in Table 1 provide the first clear observational evidence of gas of a parent molecular cloud not at rest with respect to a dissociation front.

We now consider how consistent is a standard model of a PDR, such as that in Abgrall et al. 1992, with the linewidth data in Table 1, taken in conjunction with the emissivity in the S(1) line reported in Lemaire et al. 1996 for the region observed. Velocity gradients are not included in present PDR models and are ignored here. Standard PDR models yield the following picture for a dense cloud in the presence of a high ambient radiation field. Starting from the irradiated surface of the molecular cloud and moving towards regions of increasing optical depth, there is initially a zone of hot H atoms and HII, a zone of hot H atoms mixed with $\sim$ 10% H_2, a proportion of which is vibrationally excited, a zone in which HI, CII, and H_2 coexist and a zone in which CI and CO coexist.

How does this picture tally with the data of Table 1? Consider first the linewidths of species shown in Table 1. Interpreting linewidths purely in terms of kinetic temperature for H and H_2, H atoms are at an apparent temperature of 800 K and H_2 at 500±70 K (see above). For comparison, Moutou et al. 1998 recently determined a kinetic temperature for this region of $\sim$ 400 K, where this figure was derived from a Boltzmann plot involving H_2 rotational lines. Data of Moutou et al. were obtained using the SWS on ISO centered at 27″W 34″N of HD 200775, with a 14″×20″ beam. These data provide valuable independent confirmation of our present results, albeit that the ISO data refer to a much larger region. Returning to the data of Table 1, linewidths of the other species, save perhaps that of CI, are too large to be interpreted purely in terms of thermal motion. PDR models show that emission from ^{12}CO J=6-5 probably has a contribution to the linewidth from optical depth, as well as turbulence, and therefore cannot be used to estimate temperature.

Table 1. Velocities in v_{lsr}, widths and corresponding positions for HI data (Fuente et al. 1996), H_2 (present work), CII, CI and CO (6-5, 3-2) emission data (Gerin et al. 1998) and ^{13}CO (1-0) emission data (Fuente et al. 1998a). Positions are given relative to that of HD 200775, the illuminating star. Linewidths in the second column are values at full-width-half-maximum, and may be assigned errors not exceeding ± 10%

Species observed	Linewidth (km s^{-1})	Velocity (km s^{-1})	Position	Beam size
HI	6	4 to 5	20″W 30″N	14″
H_2	3.4	3.75± 0.25	32″W 35.5″N	5″
CII	3.4	2.8± 0.1	20″W 30″N	45″
CI	1.2	2.25± 0.3	40″W 40″N	15″
^{12}CO(6-5)	1.5	2.6± 0.3	30″W 40″N	10″
^{13}CO(3-2)	0.6	2.5± 0.3	30″W 40″N	20″
^{13}CO(1-0)	-	1.9± 0.5	20″W 40″N	24″

The linewidth of CII may be partially attributed to turbulence and velocity fields, noting the large beam associated with these observations (Gerin et al. 1998). The linewidth of CI in purely thermal terms is equivalent to a temperature of $\sim$ 380 K. PDR models, as described below, however require that the temperature of CI be $\sim$ 100 K. We note that the observed linewidth may be made consistent with a temperature of 100 K by introducing a turbulent linewidth of 1 km s^{-1} ($\sim$ 0.015 cm^{-1}). The figure of 1 km s^{-1} is typical of PDRs and is in keeping with the linewidth of the ^{12}CO(6-5) emission and the rather lower figure for ^{13}CO(3-2) emission shown in Table 1. ^{13}CO emission is formed deep within the PDR, in much cooler regions and the linewidth is dominated by turbulent rather than thermal motions. CI is at least partly co-extensive with vibrationally excited H_2 and the same turbulent contribution to the H_2 linewidth would yield a temperature of $\sim$ 450 K for H_2 and $\sim$ 750 K for HI.

Concentrating on the outer part of the PDR, the observational data therefore require that the HI zone should be at 750 K, the H_2 zone at 450 K and the CI zone at 100 K. A PDR model should also yield the observed emissivity in the S(1) v=1-0 line. This has been measured to have a maximum value of 3.7(±0.4)x10^{-7} Wm^{-2} sr^{-1} (Lemaire et al. 1996) in a 1″ beam, within the region observed here. The linewidth which we report in Figs. 2 and 3 is a superposition of linewidths originating from a number of different regions, dominated by the brightest emission within the 5 arcsec beam of the observations. The emissivity with which to associate the kinetic temperature of 450 K is clearly less than the maximum value quoted above. In order to estimate the relevant emissivity, the total flux contained with the 5 arcsec circular aperture (79 pixels) was computed from the data reported in Lemaire et al. 1996. The flux in the brightest part of the filament was then computed, in a 2x2 pixel region. Taking account of the small additional influence of the underlying continuum, the effective dilution of the intensity in our 5 arcsec aperture was found to be through a factor of 2.75± 0.25. On this basis the observed temperature should be associated with a brightness of $\sim$ 1.4(±0.3)x10^{-7} Wm^{-2} sr^{-1}.

Emissivities have been calculated for a variety of conditions with an appropriate enhancement of the UV radiation field, G_0, of 10^4 over the average interstellar field (Gerin et al. 1998; Mathis et al. 1983), using a 1-D code based upon that in Abgrall et al. 1992. This model includes computation of the thermal balance and thus of the kinetic temperature of the H_2 emitting zone. Both isochoric (uniform density) and isobaric (uniform pressure) models have been used. Isochoric models require a high number density (n = n_H + 2n_{H_2}), of several times 10^6 cm^{-3} in order to achieve low temperatures and high emissivities. For example n=5x10^6 cm^{-3} gives an emissivity in the S(1) line of 2.6x10^{-7} Wm^{-2} sr^{-1} generated within a region of kinetic temperature $\sim$ 660 K, rather higher than deduced from observations. Isobaric models yield comparable results. For example a pressure of 5x10^8 Kcm^{-3} yields a (somewhat lower) emissivity of 8.3x10^{-8} Wm^{-2} sr^{-1} in the S(1) v=1-0 line. The temperature in the region from which the majority of the emission emanates is $\sim$ 550 K, in substantial agreement with observation. The corresponding particle number density (=n_H + n_{H_2}+n_{He}) is 9x10^5 cm^{-3}. The results of this isobaric model are illustrated in Fig. 4, which shows the integrated emissivity of the S(1) and S(2) v=1-0 lines as a function of distance into the PDR. The kinetic temperature is shown as a solid line. CI emission is found where the temperature is 85 K, again in agreement with observation, given 1 km s^{-1} of turbulence.

In connection with our calculations, we note that models generally show v=1-0 S(1)line emissivities in the neighbourhood of $\sim$ 10^{-7} Wm^{-2} sr^{-1} for G_0=10^4 and a number density of 10^6 cm^{-3} (e.g. Burton et al. 1992; Sternberg & Dalgarno 1989). Sternberg & Dalgarno 1989 gives a temperature in the H_2 emitting region of a few hundred K for these conditions. Results in Draine & Bertoldi 1996 (DB96), for model "Qw30", again for G_0 = 10^4 and a number density of 10^6 cm^{-3}, show a v=1-0 S(1) line emissivity of 1.4x10^{-7} Wm^{-2} sr^{-1} in good agreement with our present observations. DB96 does not however examine the thermal balance in the PDR and this model assumed our observed temperature in the emitting region of $\sim$ 500 K.

Values mentioned above of number density or of pressure (or temperature x density) may be compared with results reported elsewhere for NGC 7023. It is not material to the present discussion whether the isochoric or isobaric definition of number density is adopted. HCN measurements of Fuente et al. 1993 suggest densities of 10^5 cm^{-3} in the gas in this region. Deeper into the PDR, CO measurements suggest densities below 10^4 cm^{-3}. Martini et al. 1997 suggest a mixture of high and low densities in order to reproduce data for H_2 emission at their 'position 1', 40″W 34″N of HD 200775, close to that of the present work. This is compatible with an isobaric model, since an isobaric model corresponds to a mixture of number densities as temperature changes. Results in Martini et al. 1997 yield number densities with values between 10^5 cm^{-3} and 10^6 cm^{-3} and are thus in agreement with present estimates.

A further constraint on any model arises from the observed S(1)v=1-0/S(2)v=1-0 line ratio. Martini et al. 1997 observe a value of 2.7±0.3, and the value found in observations of Lemaire

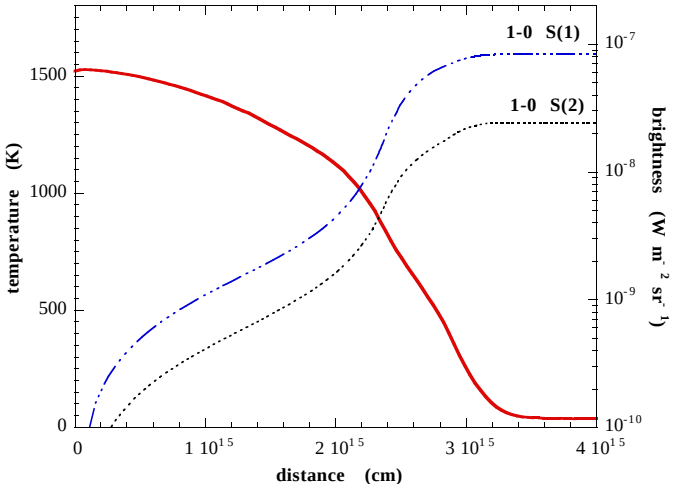

Fig. 4. The computed integrated emissivity in v=1-0 S(1) (chained line) and in v=1-0 S(2) (dotted line) as a function of position within a plane parallel slab of gas, irradiated by a VUV field of 10^4 times the mean intensity defined in the ISM, for a pressure of 5x10^8 Kcm^{-3}, using isobaric conditions. The kinetic temperature in the medium is shown as a solid line.

et al. 1996 is also 2.7±0.3. The isobaric model in Fig. 4 gives a ratio of 3.4, and the isochoric model, with a number density of 5x10^6 cm^{-3}, gives a ratio of 4.2. A lower pressure (isobaric) model, for example of between 1x10^8 and 2x10^8 Kcm^{-3}, reproduces both the temperature and S(1)v=1-0/S(2)v=1-0 line ratio, but fails to yield sufficient S(1) line emissivity. The model of DB96, referred to above, gives a S(1)/S(2) ratio of 3.3.

One reason that PDR models are not wholly successful in reproducing our observational data may rest in the difficulty in determining the thermal balance and thus the temperatures of the emitting regions (Draine & Bertoldi 1998). Models are also geometrically too simple: the medium is not composed, on a few arcsec scale, of a one-dimensional slab. The observations of Lemaire et al. 1996 show the presence of bright knots embedded in regions of lower emissivity. In addition, spectrally (R∼ 2000) and spatially resolved data, taken using the BEAR instrument on the CFHT and presently being analyzed, show rapid spatial variations in the H_2 spectrum, indicative of rapidly changing physical conditions.

The successes and failures of current models apart, our demonstration of relative flow requires a consideration of time-dependent effects within the PDR in NGC 7023. Advection of warm material from the outer part of the PDR into the cooler part, say, would increase the temperature deeper into the PDR over the value estimated purely from the atomic and molecular microphysics (e.g. Sternberg & Dalgarno 1989). The rate of the increase of temperature in the PDR depends on the advection velocity and local temperature gradient. This problem can therefore only be addressed in models which include flows (Hollenbach & Tielens 1999). The advection of irradiated material in the PDR has not been considered in the context of a pure PDR, although it has been studied for a combined PDR and ionization front in the presence of an expanding HII region (Bertoldi & Draine 1996; see also Störzer & Hollenbach 1998; Hollenbach & Tielens 1999).

A consideration of timescales also supports the need for time-dependent models of PDRs. The size of the H_2 emission zone is typically ∼ 3x10^{15} cm in our models. With a dissociation front (projected) velocity of 1 km s^{-1}, as suggested by the data in Table 1, a characteristic timescale for the PDR is 10^3 years. According to results reported for the time-dependent theory of Goldshmidt & Sternberg 1995, whose work does not include advective mixing, a PDR with a number density of 7x10^5 cm^{-3} would require several thousand years to reach a steady state. Non-steady state phenomena are shown in Goldshmidt & Sternberg 1995 to enhance H_2 emission line intensities. Some of the present difficulties would be resolved if pre-steady state times could be shown to yield the observed S(1) v=1-0 line emissivity and the S(1)/S(2) line ratio in gas with low kinetic temperature.

Notwithstanding the possible influence of time dependence in the PDR, there appears to be a general enhancement of density at the border of the molecular region, where the H_2 emission originates. This may be associated with the velocity gradient in the molecular zone, exemplified by the velocity shift between HI, H_2 and CO. The velocity of the star is too poorly known to determine the motion of H_2 (or other species) relative to the star (Finkenzeller & Jankovics 1984; Turon et al. 1993). An expanding HII zone around HD 200775 (Denizman et al. 1994; Lemaire et al. 1996) would compress the gas at the edges of the PDR, as discussed recently in the context of PDRs in Störzer & Hollenbach 1998. However the presence of an expanding HII region would not appear to be consistent with current estimates of the age of HD 200775, which lie in excess of 10^6 years (e.g. Fuente et al. 1998b). One may add that HD 200775 is known to belong to the class of Herbig AeBe stars (van den Ancker et al. 1998). It has a measured IR excess, indicative of circumstellar material (Corcoran & Ray 1998), and a high measured mass loss rate (Nisini et al. 1995). Together these indicate the presence of a stellar wind which could exert some influence at the interface with the molecular zone and contribute to compression of material in this region.

In conclusion, it is evident that NGC 7023 is a dynamically interesting region. As an archetype of a young star formation region, it continues to be worthy of further detailed study. It would for example be of considerable value if a velocity, accurate to within 1 or 2 km s^{-1}, could be established for HD 200775. The present velocity of the star is known only within an accuracy of ±6 km s^{-1} and an accurate value would enable us to establish the motion of the surrounding gas relative to the star. In addition to the BEAR data mentioned above, high resolution (R∼ 25,000) data, again obtained using the BEAR instrument on the CFHT, are presently being analyzed and promise to shed further light on the dynamics of NGC 7023 and introduce further constraints on PDR models.

Acknowledgements. We should like to thank the Director and Staff of the Canada-France-Hawaii Telescope Corporation for making possible the observations reported in this paper. We should also like to acknowledge the assistance of the Particle Physics and Astronomy Research Council (UK) and the CNRS for financial assistance for one of us (DF).

We also thank Drs. F. and M. Spite, Observatoire de Paris-Meudon, for their help in relating earth and heliocentric velocities and v_{lsr}. We are also grateful to Drs.J.Y.Mandin and V.Dana, Laboratoire de Physique Moléculaire et Applications, Paris VI, for their help with the fitting shown in Fig. 3.

References

Abgrall H., Le Bourlot J., Pineau des Forêts. G., Roueff E., Flower D.R. and Heck L., 1992 A&A 253, 525

Abrams M.C., David S.P., Rao M.L.P., Engelman R. and Brault J.W.,1994, ApJ Suppl.Ser. 93, 351

Bertoldi F. and Draine B.T., 1996 ApJ 458, 222

Black J.H. and van Dishoeck E.F., 1987, ApJ 322, 412

Bragg S.L., Brault J.W. and Smith W.H., 1982, ApJ 263, 999

Burton M.G., Geballe T.R., Brand P.W.J.L. et al. 1990, ApJ 352, 625

Burton M.G., Hollenbach D.R., Tielens A.G.G.M. 1992, ApJ 399, 563

Césarsky D., Lequeux J., Abergel A., Perault M., Palazzi E., Madden S. and Tran D., 1996, A&A 315, L305

Corcoran M., Ray T.P., 1998 A&A 331, 147

Denizman L., Koktay T., Kocer D., Eker T., Hack M., 1994, The Nature and Evolutionary Status of Herbig Ae/Be Stars, ASP Conference Series, vol. 62, Pik Sin The, Perez MR, van der Heuvel EPJ (eds.)

Draine B.T., Bertoldi F., 1996, ApJ 468. 269

Draine B.T., Bertoldi F. in "The Universe as seen by ISO", Paris Oct.1998, eds. Cox P., Demuyt V. and Kessler M.

Federman S.R., Knauth D.C., Lambert D.L. and Anderson B.G., 1997, ApJ 489, 758

Finkenzeller U. and Jankovics I., 1984, A&A Supp.Ser. 57, 285

Fuente A., Martin-Pintado J., Cernicharo J., Brouillet N., & Duvert G., 1992, A&A 260, 341

Fuente A., Martin-Pintado J., Cernicharo J. & Bachiller R., 1993, A&A 276, 43

Fuente A., Martin-Pintado J., Neri R., Rogers C. and Moriarty-Scheiven G., 1996, A&A 310, 286

Fuente A. and Martin-Pintado J., 1997 ApJ 477, L107

Fuente A., Martin-Pintado J., Rodriguez-Franco A. and Moriarty-Schieven G.D., 1998a, A&A 339, 575

Fuente A., Martin-Pintado J., Bachiller R., Neri R. and Palla F., 1998b, A&A 334, 253

Gerin M, Phillips T.G., Keene J., Betz A.L. and Boreiko R.T., 1998 ApJ 500, 329

Goldshmidt O. and Sterberg A., 1995 ApJ 439, 256

Hollenbach D.R., Tielens A.G.G.M., 1999 Rev.Mod.Phys. 71, 173

Laureijs R.J., Acosta-Pulido J., Abraham P. et al. 1996, A&A 315, L313

Lemaire J.L., Field D., Gerin M., Leach S., Pineau des Forêts G., Rostas F. and Rouan D., 1996, A&A 308, 895

Maillard, J.P. and Michel, G. 1982, A high Resolution Fourier Transform Spectrometer for the Cassegrain focus at the CFH Telescope, in Instrumentation for Astronomy with large Optical Telescopes, IAU Coll. No 67, Colin M. Humphries, ed., D. Reidel Pub., vol. 92, p.213–222: see also http://ftp.cfht.hawaii.edu/manuals/fts/fts man.html.

Martini P. Sellgren K and Hora J.L. 1997, ApJ 484, 296

Mathis J.S., Mezger P.G. and Panagia N., 1983, A&A 182, 212

Moutou C., Verstraete L., Sellgren K. and Léger A., in "The Universe as seen by ISO", Paris Oct.1998, eds. Cox P., Demuyt V. and Kessler M.

Murphy J., Dring A., Henry, R.C.,Kruk, J.W., Blair, W.P., Kimble, R.A. and Durrance S.T. 1993 ApJ 408, L97

Nisini B., Milillo A., Saraceno P., Vitali F., 1995 A&A 302, 169

Oliva E. and Origlia L., 1992, A&A 254, 466

Rogers C., Heyer M.H. and Dewdney P.E., 1995 ApJ 442, 694

Sellgren K 1983, A.J. 88, 985

Sellgren K, Werner M.W. and Dinerstein H.L., 1992, ApJ 407, 238

Sternberg A., Dalgarno A., 1989, ApJ 338, 197

Störzer H. and Hollenbach D.J. 1998, ApJ , 495, 853.

Turon C., Egret D., Gomez A. et al., 1993, The Hipparchos Input Catalogue ESA SP-1136, vol. 5

van den Ancker M.E., de Winter D., Tjin A Djie H.R.E., 1998 A&A 330, 145 (1998)

Witt A.N., Petersohn J.K., Bohlin R.C., O'Connell R.W., Roberts M.S., Smith A.M. and Stecher T.P., 1992, ApJ 395, L5

Witt A.N., Petersohn J.K., Holberg J.B., Murphy J., Dring A. and Henry, R.C., 1993, ApJ 410, 714